Pattern Recognition, Vol. 26, No. 5, pp. 683 686, 1993
Printed in Great Britain

0031-3203/93 $6.00 + .00
Pergamon Press Ltd

IMPROVED MOMENT INVARIANTS FOR SHAPE DISCRIMINATION

CHAUR-CHIN CHEN
Department of Computer Science, National Tsing Hua University, Hsinchu 300, Taiwan, Republic of China

(*Received* 27 *January* 1992; *in revised form* 18 *September* 1992; *received for publication* 1 *October* 1992)

Abstract—Moment invariants have been frequently used as features for shape recognition. They are computed based on the information provided by both the shape boundary and its interior region. Although several fast algorithms for computing traditional moment invariants have been proposed, none has ever shown the theoretical results of moment invariants computed based on the shape boundary only. This paper proposes improved moment invariants computed using the shape boundary only, which tremendously reduces computations. The new moment invariants, called improved moment invariants are mathematically proved to be invariant to scaling, translation, and rotation. Graphical plots of the first two improved moment invariants for six country maps and four industrial tools using improved moment invariants are also given. The results suggest that improved moment invariants can be used as effective features for shape discrimination or recognition.

Improved moment invariants   Traditional moment invariants   Shape feature extraction
Shape recognition

1. INTRODUCTION

The use of moment invariants as features for shape recognition and identification can be found elsewhere[1-4] since they were first proposed by Hu.[5] It is well known that the moments, proposed by Hu,[5] must be computed over all pixels including the shape boundary and its associated interior part, which is time consuming. Although some fast algorithms of computing moment invariants were proposed in the recent literature [6,7] and some scaling error was mentioned,[8] none of them have discovered the case when the moments are computed only along the shape boundary.

This paper proposes modified moment invariants based on the shape boundary only to reduce computations. The new moment invariants, called improved moment invariants, are quite similar to the previous ones, but require only the computations along the shape boundary. The two provided examples suggest that improved moment invariants are a good set of discriminant shape features.[9]

2. TRADITIONAL MOMENT INVARIANTS

Let $f(x, y)$ be 1 over a closed and bounded region R and 0 otherwise. Define the (p, q)th moment as

$$m_{pq} = \iint_R x^p y^q f(x, y)\,dx\,dy, \quad \text{for } p, q = 0, 1, 2, \ldots. \tag{1}$$

The central moments can be expressed as

$$\mu_{pq} = \iint_R (x - \bar{x})^p (y - \bar{y})^q f(x, y)\,dx\,dy$$

$$\text{where } \bar{x} = \frac{m_{10}}{m_{00}}, \quad \bar{y} = \frac{m_{01}}{m_{00}}. \tag{2}$$

For a digital image, equation (1) becomes

$$\mu_{pq} = \sum\sum_{(x,y)\in R} (x - \bar{x})^p (y - \bar{y})^q. \tag{3}$$

It can be easily verified[4] that the central moments up to the order $p + q \leq 3$ may be computed by the following formulas:

$$\begin{aligned}
&\mu_{00} = m_{00}, && \mu_{11} = m_{11} - \bar{y}m_{10} \\
&\mu_{10} = 0, && \mu_{30} = m_{30} - 3\bar{x}m_{20} + 2\bar{x}^2 m_{10} \\
&\mu_{01} = 0, && \mu_{12} = m_{12} - 2\bar{y}m_{11} - \bar{x}m_{02} + 2\bar{y}^2 m_{10} \\
&\mu_{20} = m_{20} - \bar{x}m_{10}, && \mu_{21} = m_{21} - 2\bar{x}m_{11} - \bar{y}m_{20} + 2\bar{x}^2 m_{01} \\
&\mu_{02} = m_{02} - \bar{y}m_{01}, && \mu_{03} = m_{03} - 3\bar{y}m_{02} + 2\bar{y}^2 m_{01}.
\end{aligned} \tag{4}$$

The central moments are invariant to translation. They can also be normalized to be invariant to a scaling change by the following formula. The quantities in equation (5) are called normalized central moments

$$\eta_{pq} = \frac{\mu_{pq}}{\mu_{00}{}^{\gamma}} \text{ where } \gamma = \frac{p+q}{2} + 1, \quad \text{for } p + q = 2, 3, \ldots. \tag{5}$$

The following moment invariants were derived by Hu[5] and were frequently used as features for shape recognition:

$$\phi_1 = \eta_{20} + \eta_{02}$$

$$\phi_2 = (\eta_{20} - \eta_{02})^2 + 4\eta_{11}^2$$

$$\phi_3 = (\eta_{30} - 3\eta_{12})^2 + (\eta_{03} - 3\eta_{21})^2$$

$$\phi_4 = (\eta_{30} + \eta_{12})^2 + (\eta_{03} + \eta_{21})^2$$

$$\phi_5 = (\eta_{30} - 3\eta_{12})(\eta_{30} + \eta_{12})[(\eta_{30} + \eta_{12})^2 - 3(\eta_{21} + \eta_{03})^2] + (3\eta_{21} - \eta_{03})(\eta_{21} + \eta_{03}) \times [3(\eta_{30} + \eta_{12})^2 - (\eta_{21} + \eta_{03})^2]$$

$$\phi_6 = (\eta_{20} - \eta_{02})[(\eta_{30} + \eta_{12})^2 - (\eta_{21} + \eta_{03})^2] + 4\eta_{11}(\eta_{30} + \eta_{12})(\eta_{21} + \eta_{03})$$

$$\phi_7 = (3\eta_{21} - \eta_{03})(\eta_{30} + \eta_{12})[(\eta_{30} + \eta_{12})^2 - 3(\eta_{21} + \eta_{03})^2] + (3\eta_{12} - \eta_{30})(\eta_{21} + \eta_{03}) \times [3(\eta_{30} + \eta_{12})^2 - (\eta_{21} + \eta_{03})^2]. \quad (6)$$

The quantities, ϕ_i, $1 \le i \le 7$, were shown to be invariant to scaling, translation, and rotation by Hu.[5] However, they are computed over the shape boundary associated with its interior part. The next section provides a significant improvement such that the moment invariants are computed based only on the shape boundary, and hence we call them improved moment invariants.

3. IMPROVED MOMENT INVARIANTS

We modified the moment definition in equation (1) using the shape boundary only. For convenience, we used the same notation to express the modified moments

$$m_{pq} = \int_C x^p y^q \, ds, \quad \text{for } p, q = 0, 1, 2, 3, \ldots \quad (7)$$

where $\int_C$ is a line integral along the curve C, $ds = \sqrt{((dx)^2 + (dy)^2)}$, the modified central moments can be similarly defined as

$$\mu_{pq} = \int_C (x - \bar{x})^p (y - \bar{y})^q \, ds, \text{ where } \bar{x} = \frac{m_{10}}{m_{00}}, \quad \bar{y} = \frac{m_{01}}{m_{00}}. \quad (8)$$

For a digital shape, equation (8) becomes

$$\mu_{pq} = \sum_{(x,y) \in C} (x - \bar{x})^p (y - \bar{y})^q. \quad (9)$$

It is obvious that the modified central moments are invariant to translation. The following two theorems show how to normalize the modified central moments such that they are also scaling-invariant, and provide an alternative and intuitive proof of rotation invariance for the improved moment invariants defined in equation (7) and normalized by using equation (10) given next.

Theorem 1. For μ_{pq} defined in equation (8)

$$\eta'_{pq} = \frac{\mu_{pq}}{(\mu_{00})^{p+q+1}} \text{ is scaling-invariant for } p + q = 2, 3, \ldots. \quad (10)$$

Proof. Suppose C is a smooth curve in the plane, C' is the curve obtained by homogeneously rescaling the coordinates by a factor r, then

$$\mu'_{pq} = \int_{C'} [x(s')]^p [y(s')]^q \, ds' = \int_C [rx(s)]^p [ry(s)]^q \, d(rs) = r^{p+q+1} \int_C [x(s)]^p [y(s)]^q \, ds = r^{p+q+1} \mu_{pq}. \quad (11)$$

Since

$$\mu_{00} = \int_C ds = |C| = \text{length of curve } C \quad (12)$$

$$\mu'_{00} = \int_{C'} ds' = |C'| = \text{length of curve } C' = r|C|. \quad (13)$$

Then, for any $r > 0$, we have

$$\frac{\mu'_{pq}}{(\mu'_{00})^{p+q+1}} = \frac{r^{p+q+1}\mu_{pq}}{r^{p+q+1}|C|^{p+q+1}} = \frac{\mu_{pq}}{(\mu_{00})^{p+q+1}}. \quad (14)$$

Thus, $\mu_{pq}/(\mu_{00})^{p+q+1}$ is invariant to a homogeneous scaling.

Theorem 2. Suppose C is a smooth curve in the plane and C' is the curve obtained by rotating C an angle θ clockwise, then

$$\phi'_i = \phi_i \quad \text{for } 1 \le i \le 7 \quad (15)$$

where ϕ'_i is defined as in equation (6) by using η'_{pq} instead of η_{pq} for $p + q = 2, 3, \ldots$.

Proof.

$$\mu'_{pq} = \int_{C'} [x(s')]^p [y(s')]^q \, ds' = \int_C \{[x(s)\cos\theta - y(s)\sin\theta]^p [y(s)\sin\theta + x(s)\cos\theta]^q\} \, ds. \quad (16)$$

Note that $ds' = ds$. We shall prove $\phi'_1 = \phi_1$ and $\phi'_2 = \phi_2$ as examples. For $3 \le j \le 7$, $\phi'_j = \phi_j$ can be similarly proved after tedious computations by using the trigonometric identities, $\cos^2\theta + \sin^2\theta = 1$, $(\cos^3\theta - 3\cos\theta\sin^2\theta)^2 + (\sin^3\theta - 3\cos^2\theta\sin\theta)^2 = 1$.

Since, the length of a plane curve is invariant under rotation, that is, $\mu'_{00} = \mu_{00}$, from equation (6), we have

$$\begin{aligned}(\mu'_{00})^3\phi'_1 &= (\mu'_{00})^3(\eta'_{20} + \eta'_{02}) \\ &= \mu'_{20} + \mu'_{02} \\ &= \int_C \{[x(s)\cos\theta - y(s)\sin\theta]^2 + [x(s)\sin\theta + y(s)\cos\theta]^2\} \, ds \\ &= \int_C \{[\cos^2\theta + \sin^2\theta][x(s)]^2 + [\cos^2\theta + \sin^2\theta][y(s)]^2\} \, ds \\ &= \int_C \{[x(s)]^2 + [y(s)]^2\} \, ds \\ &= \mu_{20} + \mu_{02} = (\mu_{00})^3(\eta_{20} + \eta_{02}) = (\mu'_{00})^3\phi_1.\end{aligned} \quad (17)$$

Therefore

$$\phi'_1 = \phi_1.$$

Again from equation (6) we have

$$
\begin{aligned}
(\mu'_{00})^6\phi'_2 &= (\mu'_{00})^6[(\eta'_{20}-\eta'_{02})^2 + 4\eta'^2_{11}] \\
&= (\mu'_{20}-\mu'_{02})^2 + 4\mu'^2_{11} \\
&= [\int_C \{[x(s)\cos\theta - y(s)\sin\theta]^2 \\
&\quad - [x(s)\sin\theta + y(s)\cos\theta]^2\}\,ds]^2 \\
&\quad + 4\{\int_C [x(s)\cos\theta - y(s)\sin\theta] \\
&\quad \times [x(s)\sin\theta + y(s)\cos\theta]\,ds\}^2 \\
&= [\mu_{20}\cos 2\theta - \mu_{02}\cos 2\theta - 2\mu_{11}\sin 2\theta]^2 \\
&\quad + [\mu_{20}\sin 2\theta - \mu_{02}\sin 2\theta + 2\mu_{11}\cos 2\theta]^2 \\
&= [\mu_{20}-\mu_{02}]^2 + 4\mu^2_{11} \\
&= (\mu_{00})^6[(\eta_{20}-\eta_{02})^2 + 4\eta^2_{11}] = (\mu'_{00})^6\phi_2. \qquad (18)
\end{aligned}
$$

Therefore

$$\phi'_2 = \phi_2.$$

4. EXAMPLES

The performance of our improved moment invariants were experimentally demonstrated by Chang[9] through testing five sets of shapes. This section provides two examples. Figures 3 and 4 show the plots based on the first two improved moment invariants for a set of six country maps, including Canada (c), China (n), France (f), Italy (i), Taiwan (t), and United States (u) given in Fig. 1, and for a set of industrial tools, including screwdriver (s), hammer (h), scissors (x), and pliers (p) given in Fig. 2. From the plots, the contours of France and United States are similar, and the contours of scissors and pliers are similar, which matches human visual judgement.

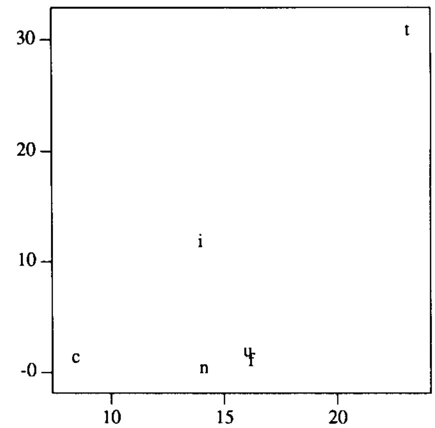

Fig. 3. Plot of country maps based on the first two improved moment invariants.

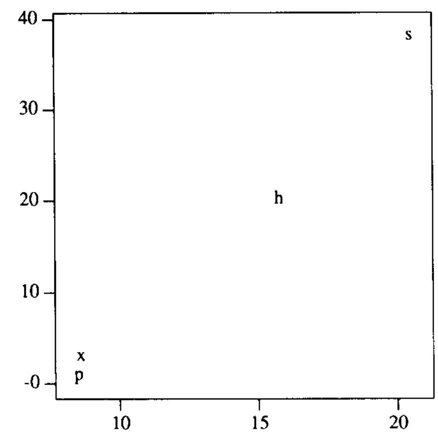

Fig. 4. Plot of industrial tools based on the first two improved moment invariants.

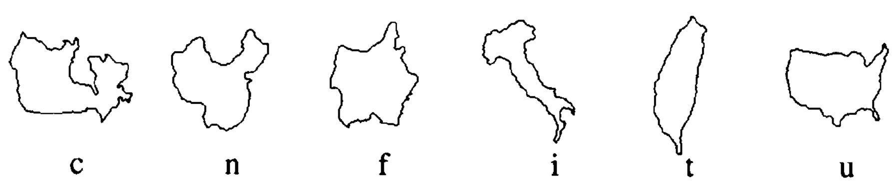

Fig. 1. Country maps: Canada, China, France, Italy, Taiwan, U.S.A.

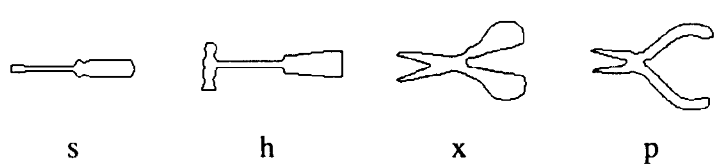

Fig. 2. Industrial tools: screwdriver, hammer, scissors, pliers.

5. CONCLUSION

We have mathematically proved that the traditional moment invariants proposed by Hu[5] can be slightly modified such that the improved moment invariants are computed only along the shape boundary, which tremendously reduces the computational efforts. The improved moment invariants can be easily computed from a chain code representation of the shape boundary.[9] The computations of seven improved moment invariants for a digital shape of size 250×250 pixels require about 0.6 s on a Sun 4/330 machine, however it requires more than 15 s for computing the traditional moment invariants. Although fast computations[1,6] of traditional moment invariants were proposed, they perform shape feature extraction from the shape "region" not from the shape boundary.

It must be mentioned that the improved moment invariants and traditional moment invariants are different shape features. It is not appropriate to say that one outperforms another on all data sets. Future work needs to compare the performance evaluation for the improved moment invariants and the traditional moment invariants.

Acknowledgement—The author appreciates the valuable comments and corrections from the reviewer which has made the paper more legible. This work was partially supported by NSC 81-0408-E007-526.

REFERENCES

1. S. A. Dudani, K. J. Breeding and R. B. McGhee, Aircraft identification by moment invariants, *IEEE Trans. Comput.* **26**, 39–46 (1977).
2. L. Gupta, Invariant planar shape recognition, *Pattern Recognition* **21**, 235–239 (1988).
3. Z. Mingfa, S. Hasani, S. Bhattarai and H. Singh, Pattern recognition with moment invariants on a machine vision system, *Pattern Recognition Lett.* **9**, 175–180 (1989).
4. Z. You and A. K. Jain, Performance evaluation of shape matching via chord length distribution, *Comput. Vision Graphics Image Process.* **28**, 85–198 (1984).
5. M. K. Hu, Visual pattern recognition by moment invariants, *IEEE Trans. Inf. Theory* **12**, 179–187 (1962).
6. B. C. Li and J. Shen, Fast computation of moment invariants, *Pattern Recognition* **24**, 807–813 (1991).
7. M. F. Zakaria, L. J. Vroomen, P. J. A. Zsombor-Murray and J. M. H. M. Van Kessel, Fast algorithm for the computation of moment invariants, *Pattern Recognition* **20**, 639–643 (1987).
8. T. H. Reiss, The revised fundamental theorem of moment invariants, *IEEE Trans. Pattern Analysis Mach. Intell.* **13**, 830–834 (1991).
9. C. S. Chang, Building an efficient 2D shape recognition system, Master's Thesis, National Tsing Hua University, Hsinchu, Taiwan, June (1991).

About the Author—CHAUR-CHIN CHEN was born in Kaohsiung, Taiwan, in 1955. He received the B.S. degree in mathematics from National Taiwan University, Taiwan, in 1977, the M.S. degrees in mathematics and computer science, in 1982 and 1984, respectively, and the Ph.D. degree in computer science in 1988, all from Michigan State University. He was a visiting research associate at Michigan State University from January to June, 1989 and is currently an Associate Professor in the Department of Computer Science at National Tsing Hua University, Taiwan. His research interests are in the areas of pattern recognition, image processing, and numerical analysis. Dr Chen is a member of the IEEE Computer Society, the Pattern Recognition Society, and the Association for Computing Machinery.